

Stabilization of sawteeth in tokamaks with toroidal flows

Robert G. Kleva and Parvez N. Guzdar

Institute for Plasma Research, University of Maryland, College Park, Maryland 20742-3511

(Received 20 July 2001; accepted 23 April 2002)

Sheared toroidal flows with a magnitude of the order of the sound speed are shown to stabilize sawteeth in tokamaks. In the absence of flows, tokamak equilibria in which the central safety factor q is less than unity are unstable to resistive tearing modes (resistive internal kink modes) with toroidal mode number $n=1$. As the ratio β of the plasma pressure to the magnetic field pressure increases, the growth rate of the $n=1$ mode rises because of the increasing pressure gradient. However, the addition of a toroidal flow to the equilibrium has a stabilizing effect. As the magnitude of the toroidal flow approaches the sound speed, the $n=1$ resistive tearing mode can be completely stabilized by the flow, eliminating sawteeth. © 2002 American Institute of Physics.
[DOI: 10.1063/1.1485974]

I. INTRODUCTION

The maximum temperature in tokamak experiments is often limited by the occurrence of sawteeth.^{1,2} During a discharge with sawteeth, there is a rapid, fractional drop in the central temperature, followed by a slower increase as the temperature recovers. This process then repeats periodically. The resulting time trace of the central temperature resembles sawteeth. Kadomtsev proposed a model of sawteeth³ in which Ohmic heating causes the slow rise in the central temperature and, consequently, a reduction in the plasma resistivity η . In response to the improvement in the conductivity, the central current density J_0 increases, driving the safety factor $q_0 \sim J_0^{-1}$ at the center below unity. Magnetohydrodynamic (MHD) analyses of current profiles with $q_0 < 1$ have demonstrated that such profiles are unstable to resistive tearing (resistive internal kink) mode perturbations with toroidal mode number $n=1$.^{3,4} In Kadomtsev's model, the resulting instability reconnects the reversed helical magnetic field lines around the resonant surface where $q=1$, raising q above unity everywhere. At the same time, the temperature at the center of the discharge decreases as some of the energy contained in the center is expelled outwards. In Kadomtsev's model, this entire process then repeats as the central temperature slowly rises again because of Ohmic heating, resulting in a series of periodic sawteeth in the central temperature. Numerical simulations of the MHD equations by Sykes and Wesson⁵ confirmed that magnetic field lines are reconnected at the $q=1$ resonant surface by the resistive tearing mode. Denton *et al.*⁶ then succeeded in numerically reproducing the entire time trace of the periodic sawteeth seen in tokamak experiments.

However, some of the features of Kadomtsev's model are not in accord with the experimental observations. Sawteeth can be eliminated in experiments with the use of auxiliary heating methods⁷ (ion cyclotron resonance heating and/or neutral beam heating) or by externally applied resonant magnetic perturbations.⁸ Importantly, measurements of the magnetic field profile in these experiments indicate that q_0 remains below unity during the entire period over which

sawteeth are stabilized. This observation is at odds with theoretical results which predict that current profiles with $q_0 < 1$ are unstable.³⁻⁶ This discrepancy between the experimental observations and the theoretical MHD results has prompted the creation of new models which attempt to explain this unexpected stability when $q < 1$. Explanations based upon energetic trapped particles^{9,10} and flattened current gradients with zero magnetic shear at the $q=1$ resonant surface¹¹ have been proposed.

These previous calculations of MHD stability of current profiles with $q_0 < 1$ neglected the effect of plasma flows. In slab geometry, plasma flows have been shown to have a stabilizing influence on tearing modes.¹²⁻¹⁴ In an earlier paper¹⁵ we studied the effect of a shear poloidal flow on the stability of the $n=1$ resistive internal kink (tearing) mode in current profiles with $q_0 < 1$. We demonstrated that a sheared poloidal flow can stabilize the resistive internal kink mode even though $q_0 < 1$. The $n=1$ mode is stable when the local gradient $|d\omega(r)/dr|_{r=r_1}$ in the poloidal rotation frequency $\omega(r)$ at the radius r_1 of the $q=1$ resonant surface is larger than the local gradient $|d\omega_A(r)/dr|_{r=r_1}$ in the shear Alfvén frequency $\omega_A(r) = k_{\parallel}(r)V_A$:

$$\left| \frac{d\omega(r)}{dr} \right|_{r=r_1} \geq \left| \frac{d\omega_A(r)}{dr} \right|_{r=r_1}. \quad (1)$$

Here, $k_{\parallel}(r) = R^{-1}[1 - 1/q(r)]$ is the wave number parallel to the magnetic field, $V_A = (B_{\phi}^2/4\pi\rho_m)^{1/2}$ is the Alfvén speed, r is the minor radius of the torus, R is the major radius of the torus, B_{ϕ} is the toroidal magnetic field, and ρ_m is the mass density of the plasma. The local gradient in the shear Alfvén frequency is dominated by the shear in the magnetic field. Therefore, the $n=1$ mode is stable when the local shear in the poloidal flow at the $q=1$ resonant surface is larger than the local shear in the magnetic field. This stability criterion does not at all depend on the magnitude of the plasma resistivity η or on the global details of the profiles of the rotation frequency and the current. Subsequently, toroidal flows have

been shown to have a stabilizing influence on the ideal ($\eta = 0$) internal kink mode in a large aspect ratio torus.^{16,17}

In our earlier research on poloidal flow stabilization of sawteeth,¹⁵ we considered a low β plasma, where β is the ratio of the plasma pressure P to the magnetic field pressure $B_\phi^2/8\pi$, in periodic cylindrical geometry. The plasma dynamics were described by the reduced MHD equations in which the plasma pressure is neglected. In this paper we investigate the effect of a toroidal flow on sawtooth stability for a finite β plasma in toroidal geometry. The plasma dynamics are described by the fully compressible resistive MHD equations, including an evolution equation for the plasma temperature. When the magnitude of the toroidal flow approaches the sound speed, the resulting centrifugal force becomes large enough to impact the toroidal equilibrium. We find that sheared toroidal flows with a magnitude of the order of the sound speed can completely stabilize the $n=1$ mode in tokamaks with $q_0 < 1$. In the absence of flows, the growth rate of the $n=1$ mode rises as β increases because of the increasing pressure gradient. However, the addition of a toroidal flow to the equilibrium has a stabilizing effect. As the magnitude of the flow approaches the sound speed, the $n=1$ mode can be completely stabilized, eliminating sawteeth.

The rest of this paper is organized as follows. The equations that form the basis of our numerical calculations are presented in Sec. II, and the effect of a toroidal flow on tokamak equilibrium is described. The effect of increasing β on the stability of the $n=1$ mode in flow free tokamaks is considered in Sec. III. In Sec. IV we investigate the stability of tokamak equilibria with toroidal flows. The effect of an increasing toroidal flow on the growth rate and mode structure of the $n=1$ mode is presented. The results are summarized in Sec. V.

II. TOROIDAL EQUILIBRIA WITH TOROIDAL FLOWS

Our numerical simulations of sawtooth stability in tokamaks are based on the resistive MHD equations for the magnetic field \mathbf{B} , the mass velocity \mathbf{V} , the temperature T , and the mass density ρ_m :

$$\partial \mathbf{B} / \partial t = \nabla \times (\mathbf{V} \times \mathbf{B}) + \eta \nabla^2 \mathbf{B}, \quad (2)$$

$$\partial \mathbf{U} / \partial t + \nabla \cdot (\mathbf{V} \mathbf{U}) = \mathbf{J} \times \mathbf{B} - \nabla P + \mu \nabla^2 \mathbf{U}, \quad (3)$$

$$\partial T / \partial t + \mathbf{V} \cdot \nabla T - \nabla_{\parallel} \kappa_{\parallel} \nabla_{\parallel} T = 0, \quad (4)$$

$$\partial \rho_m / \partial t + \nabla \cdot \mathbf{U} - D \nabla^2 \rho_m = 0, \quad (5)$$

where the parallel gradient $\nabla_{\parallel} = \hat{\mathbf{b}} \cdot \nabla$ with $\hat{\mathbf{b}} = \mathbf{B}/|\mathbf{B}|$, the momentum density $\mathbf{U} = \rho_m \mathbf{V}$, the pressure $P = \rho_m T$, the current $\mathbf{J} = \nabla \times \mathbf{B}$, and $\nabla \cdot (\mathbf{V} \mathbf{U}) = \mathbf{V} \cdot \nabla \mathbf{U} + (\nabla \cdot \mathbf{V}) \mathbf{U}$, for a plasma with resistivity η , viscosity μ , parallel thermal conductivity κ_{\parallel} , and diffusion coefficient D . Equations (1)–(4) are solved in toroidal geometry (R, ϕ, z) , where R is the major radial coordinate of the torus, ϕ is the toroidal angle, and z is the vertical distance along the axis of the torus, with a square conducting wall of half-width a in the poloidal plane. The equations are given in normalized units¹⁸ in which distances in R and z are normalized to a , the time t is normalized to the

Alfvén time $\tau_A \equiv a/v_A$ with v_A the Alfvén speed, the resistivity $\eta = S^{-1}$ where the Lundquist number $S \equiv \tau_r/\tau_A$ is the ratio of the resistive diffusion time τ_r to the Alfvén time, and the sound speed $c_s = \sqrt{T}$. In our simulations we consider a torus with aspect ratio $A \equiv R_0/a = 3$, where R_0 is the major radius of the torus. The magnetic field in toroidal geometry can be written in the form

$$\mathbf{B} = \nabla \psi \times \hat{\phi} / R + B_{\phi} \hat{\phi}, \quad (6)$$

where ψ is the poloidal magnetic flux and $\hat{\phi}$ is a unit vector in the ϕ direction.

Axisymmetric equilibria, independent of the toroidal angle ϕ , are obtained from Eqs. (2)–(5) by neglecting the time derivatives and the dissipative terms. In equilibrium, the net force in the momentum equation (3) must be zero:

$$-\nabla P + \mathbf{J} \times \mathbf{B} + \hat{R} \rho_m V_{\phi}^2 / R = 0, \quad (7)$$

where V_{ϕ} is the equilibrium toroidal flow velocity and \hat{R} is a unit vector in the R direction. In addition to the usual force caused by the pressure gradient and the Lorentz $\mathbf{J} \times \mathbf{B}$ force, there is an additional centrifugal force outward in the major radius because of the toroidal flow.

The rapid transport of energy along the magnetic field lines forces the equilibrium temperature to be uniform along the equilibrium magnetic field lines: $\mathbf{B} \cdot \nabla T = 0$. With expression (6) for the magnetic field, it is easy to show that this condition is satisfied if the temperature is a function $T(\psi)$ of the flux ψ .

From Eq. (2) for the magnetic field \mathbf{B} , we see that the toroidal flow V_{ϕ} will alter the equilibrium magnetic field unless the flow satisfies the equation $\nabla \times (V_{\phi} \hat{\phi} \times \mathbf{B}) = 0$. With expression (6) for the magnetic field, it is straightforward to show that the equilibrium magnetic field will not be altered by the flow if V_{ϕ} is given by the product of the major radius R and an arbitrary function $f(\psi)$ of the flux ψ . It is convenient to take $f(\psi)$ to be proportional to the sound speed $c_s = \sqrt{T(\psi)}$. Then we write V_{ϕ} in the form

$$V_{\phi} = M \frac{R}{R_{\text{axis}}} \sqrt{T(\psi)}, \quad (8)$$

where R_{axis} is the position of the magnetic axis in major radius and the Mach number M is the ratio of the toroidal flow velocity to the sound speed:

$$V_{\phi} / c_s = M \frac{R}{R_{\text{axis}}}. \quad (9)$$

The mass density ρ_m is determined by the force balance equation (7) together with expression (8) for V_{ϕ} . Let us take ρ_m to be a function of the major radius R so that the pressure $P(R, \psi) = \rho_m(R) T(\psi)$. Then the component of the force balance equation (7) parallel to the magnetic field can be written as

$$\frac{d}{dR} \rho_m = \rho_m M^2 R / R_{\text{axis}}^2. \quad (10)$$

Equation (10) can be integrated to give the equilibrium mass density

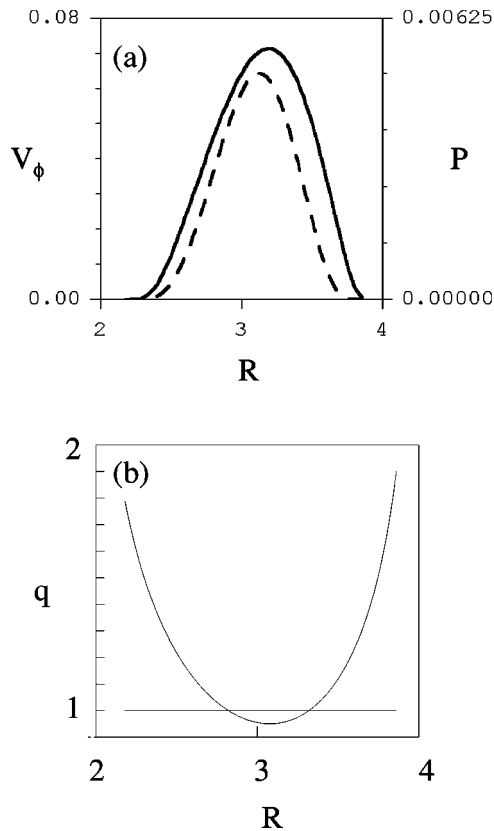


FIG. 1. Equilibrium with a sound speed toroidal flow. (a) The toroidal flow V_ϕ (solid line) and the pressure P (dashed line) are plotted as a function of the major radius R through the midplane of the torus ($z=0$) for a plasma with $\beta=1\%$. (b) The safety factor q is plotted as a function of R through the midplane ($z=0$). For reference, a line with $q=1$ is also plotted.

$$\rho_m = \exp\left(\frac{1}{2}M^2\left[\left(\frac{R}{R_{\text{axis}}}\right)^2 - 1\right]\right). \quad (11)$$

By specifying the flux ψ , the temperature $T(\psi)$ as a function of ψ , and V_ϕ and ρ_m as a function of the Mach number M through Eqs. (8) and (11), respectively, we ensure that the component of the force parallel to the magnetic field is zero in equilibrium. However, the component of the force perpendicular to the magnetic field is not, in general, zero. We obtain an axisymmetric equilibrium dynamically by solving the two-dimensional component of the MHD equations for the magnetic field (2) and the momentum (3) in the poloidal plane (R, z). The net force on the plasma perpendicular to the magnetic field generates a mass flow which alters the magnetic field and, hence, the flux ψ . The temperature is then determined through the functional form $T(\psi)$, and the toroidal flow and the mass density are determined from Eqs. (8) and (11), respectively. With the resistivity $\eta=0$, but with a nonzero viscosity μ , the system relaxes into an equilibrium in which the force balance equation (7) is satisfied. The small residual flow is damped away by the viscosity.

An example of an equilibrium with a sound speed toroidal flow ($M=1$) is shown in Fig. 1. Figure 1(a) is a plot of the toroidal flow V_ϕ (solid line) and the pressure P (dashed line) as a function of the major radius R through the midplane of the torus ($z=0$) for a plasma with $\beta=2P_0/B_{\phi 0}^2$

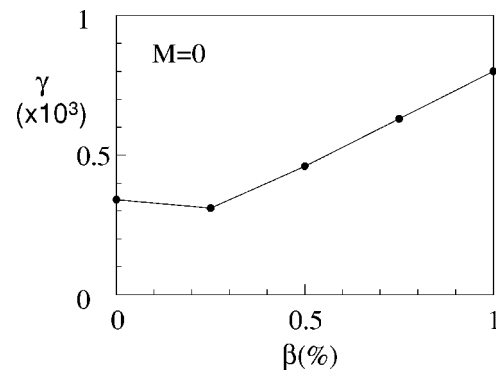


FIG. 2. Growth rate vs β in a flow free plasma. The growth rate γ of the $n=1$ mode in a flow free toroidal plasma is plotted as a function of β . The simulation results are given by the closed circles.

$=1\%$, where P_0 is the pressure at the magnetic axis and $B_{\phi 0}$ is the toroidal magnetic field at the magnetic axis. The q profile through the midplane of the torus is shown in Fig. 1(b). The minimum value of q at the magnetic axis is $q_0=0.95$. In order to eliminate any possible resonances with an $n=1$ perturbation other than the $q=1$ resonance, the current profile is chosen such that $q<2$ everywhere in the plasma.

The stability of an equilibrium with a toroidal flow to a sawtooth perturbation with toroidal mode number $n=1$ is obtained by linearizing the MHD equations (2)–(5) about the equilibrium, with all perturbed quantities varying with toroidal angle ϕ as $e^{-i\phi}$. The linearized equations are solved on a Cartesian grid in R and z . Spatial derivatives are evaluated to fourth order in the grid spacing Δ (Ref. 19), while time stepping is second-order accurate in the time step Δt with a leap frog trapezoidal scheme.²⁰ The equations are numerically integrated in time until a time-asymptotic state is reached in which the perturbed magnetic and kinetic energies vary in time as $e^{2\gamma t}$, where γ is the growth (or damping) rate of the $n=1$ sawtooth mode. Unless otherwise stated, the transport coefficients $\eta=\mu=D=3\times 10^{-5}$, and the parallel thermal conduction $\kappa_{\parallel}=1$.

III. SAWTOOTH STABILITY IN FLOW FREE FINITE β TOROIDAL PLASMAS

Before investigating the effect of toroidal flows on the stability of sawteeth, we first consider the effect of finite (nonzero) plasma pressure on sawtooth stability in flow-free toroidal plasmas. Figure 2 is a plot of the growth rate γ of an $n=1$ perturbation as a function of β in a flow-free plasma ($M=0$) with $q_0=0.95$. When the plasma pressure is zero ($\beta=0$), the equilibrium current gradient is the only source of free energy that can drive instabilities. In this current profile with $q_0<1$, an $n=1$ perturbation is unstable with a growth rate $\gamma=3.5\times 10^{-4}\tau_A^{-1}$. As β increases in magnitude from zero, the plasma pressure is no longer negligible and the growth rate of the perturbation increases monotonically with β . When β reaches 1%, the growth rate $\gamma=8\times 10^{-4}\tau_A^{-1}$, more than twice as large as the growth rate in a pressureless plasma with $\beta=0$. The plasma pressure is the dominant source of free energy when $\beta=1\%$.

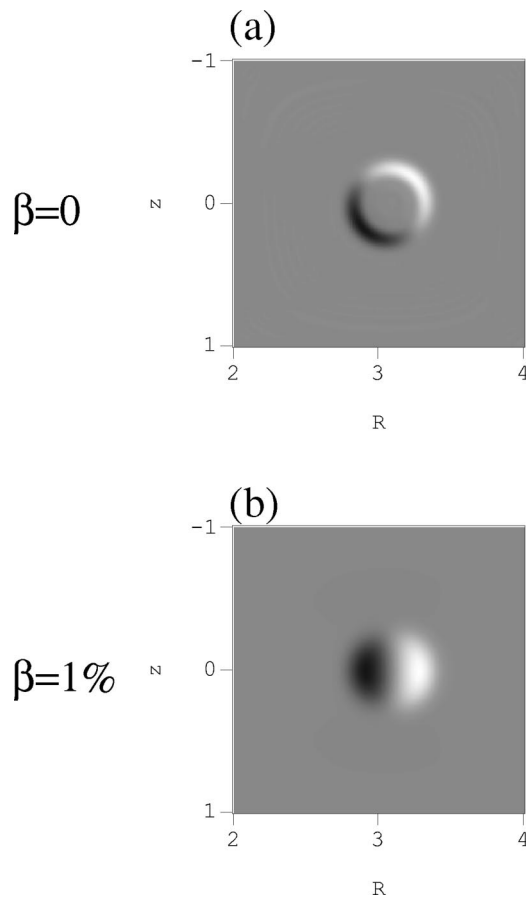


FIG. 3. Mode structure with increasing β . The real part of the pressure perturbation of the $n=1$ mode is plotted in the poloidal plane (R, z) for $\beta =$ (a) 0 and (b) 1%. The light area is the region where the pressure perturbation is positive, while the region of negative perturbed pressure is dark.

The effect of finite β on the structure of the growing pressure perturbation is shown in Fig. 3. Figure 3 is a plot of the real part of the pressure perturbation in the poloidal plane (R, z) when $\beta =$ (a) 0 and (b) 1%. The light area is the region where the pressure perturbation is positive, while the region of negative perturbed pressure is dark. In both cases the perturbation consists of two lobes. There is one lobe in which the pressure perturbation is positive and one lobe in which it is negative, so that the perturbation is proportional to $\sin(\theta + \alpha)$ where θ is the poloidal angle and α is an arbitrary phase shift. When $\beta=0$ the perturbation is localized around the flux surface where $q=1$, while when β is large the perturbation extends inward from the $q=1$ surface to the magnetic axis.

IV. STABILIZATION OF SAWTEETH BY TOROIDAL FLOWS

Consider now the effect of a toroidal flow on the stability of the $n=1$ mode in a toroidal plasma with central safety factor $q_0 < 1$. Figure 4 is a plot of the growth rate γ of an $n=1$ perturbation as a function of the Mach number M of the toroidal flow, for a toroidal equilibrium with $q_0=0.95$ and $\beta=1\%$. The results shown in Fig. 4 demonstrate that the flow has a stabilizing effect on the $n=1$ mode. A toroidal flow of one-tenth of the sound speed reduces the growth rate

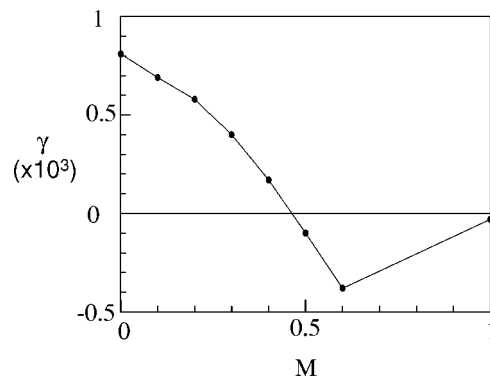


FIG. 4. Growth rate vs flow speed. The growth rate γ of the $n=1$ mode in a toroidal plasma with $\beta=1\%$ is plotted as a function of the Mach number M of the toroidal flow. The simulation results are given by the closed circles.

of the mode by about 15% compared to the growth rate in a flow-free plasma. As the magnitude of the toroidal flow increases, the growth rate of the $n=1$ mode continues to decrease. When the toroidal flow speed increases to four-tenths of the sound speed, the growth rate is five times smaller than the growth rate in a flow-free plasma. The mode is completely stabilized by the toroidal flow when the flow speed increases to one-half of the sound speed. And the mode remains stable as the flow speed increases to the sound speed.

The change in the structure of the $n=1$ mode as the toroidal flow velocity increases is displayed in Fig. 5. Figure 5 is a plot of the real part of the pressure perturbation in the poloidal plane. When the magnitude of the toroidal flow is 20% of the sound speed [Fig. 5(a)], the pressure perturbation consists of two lobes as in the flow free case [Fig. 3(b)], but the lobes are now twisted in the poloidal plane by the toroidal flow. The twisted lobes rotate in the poloidal plane around the magnetic axis. Since the structure of the $n=1$ mode is resonant with the pitch of the helical magnetic field lines at the $q=1$ magnetic flux surface, the shear in the toroidal flow twists and shears the mode in the poloidal plane. As the magnitude of the toroidal flow velocity increases, the lobes are twisted to an increasing extent [Fig. 5(b), $M=0.4$] until the $n=1$ mode is completely stabilized [Fig. 5(c), $M=0.5$].

The results in Fig. 4 describe the stabilizing influence of a toroidal flow on the $n=1$ resistive kink mode in a plasma with transport coefficients $\eta = \mu = D = 3 \times 10^{-5}$. The effect on stability of reducing the magnitude of the transport coefficients is shown in Fig. 6. The solid curve Fig. 6 is a plot of the growth rate γ of an $n=1$ perturbation as a function of the Mach number M of the toroidal flow, for a plasma equilibrium identical to that used in Fig. 4 except that $\eta = \mu = D = 2 \times 10^{-5}$. As a comparison, the stability curve in Fig. 4 for $\eta = \mu = D = 3 \times 10^{-5}$ is redrawn as the dashed line in Fig. 6. For a flow free plasma ($M=0$), the growth rate increases from $\gamma = 8.1 \times 10^{-4}$ when $\eta = \mu = D = 3 \times 10^{-5}$ to $\gamma = 9.4 \times 10^{-4}$ when $\eta = \mu = D = 2 \times 10^{-5}$. We have further reduced the magnitude of the transport coefficients in a flow free plasma and find that the growth rate reaches a maximum value of $\gamma = 1.2 \times 10^{-3}$ when $\eta = \mu = D = 5 \times 10^{-6}$. As the magnitude of the transport coefficients is reduced below

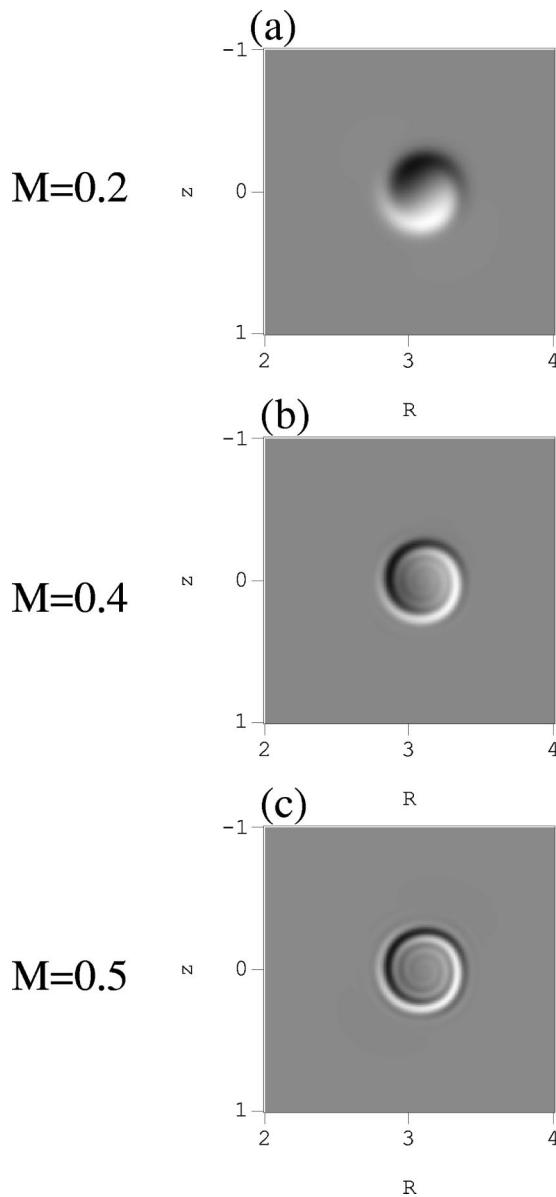


FIG. 5. Mode structure with increasing flow speed. The real part of the pressure perturbation of the $n=1$ mode is plotted in the poloidal plane (R, z) for Mach number $M=(a)$ 0.2, (b) 0.4, and (c) 0.5. The light area is the region where the pressure perturbation is positive, while the region of negative perturbed pressure is dark.

5×10^{-6} , the growth rate of the $n=1$ mode decreases. An analogous behavior has been observed in the stability of tearing modes in a cylindrical plasma.²¹ As η increases in magnitude from zero, the growth rate γ of tearing modes increases reaching a maximum value γ_0 at some η_0 . As η increases beyond η_0 , the growth rate decreases. For small $\eta < \eta_0$, the equilibrium current is nearly constant over the narrow resistive current layer around the resonant surface of the tearing mode, and the growth rate of the tearing mode scales as $\eta^{3/5}$. However, when $\eta > \eta_0$ the resonant current layer is broader and the equilibrium current varies significantly within the layer. The growth rate then decreases with increasing η . In our toroidal $n=1$ simulations, the equilibrium pressure and current profiles vary across the resonant layer around the $q=1$ surface unless η is very small. As the

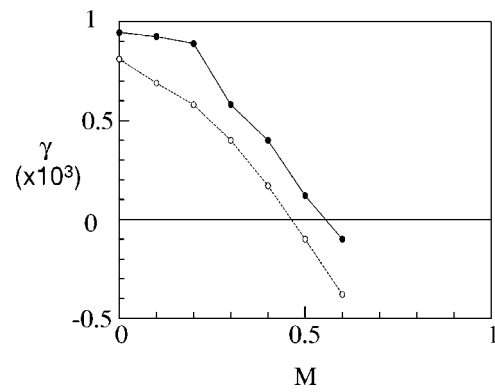


FIG. 6. Transport coefficients. The growth rate γ of the $n=1$ mode in a toroidal plasma with $\beta=1\%$ is plotted as a function of the Mach number M of the toroidal flow when $\eta=\mu=D=2 \times 10^{-5}$ (solid curve) and $\eta=\mu=D=3 \times 10^{-5}$ (dashed curve). The simulation results are given by the circles.

magnitude of the toroidal flow in Fig. 6 increases when $\eta=\mu=D=2 \times 10^{-5}$, the growth rate of the $n=1$ mode decreases. However, because the flow free growth rate when $\eta=\mu=D=2 \times 10^{-5}$ is a little larger than when $\eta=\mu=D=3 \times 10^{-5}$, the magnitude of the toroidal flow required for complete stabilization is a little larger.

V. SUMMARY

Sheared toroidal flows have a stabilizing influence on $n=1$ sawteeth in finite β tokamaks. As the magnitude of the toroidal flow increases in a tokamak plasma with $q < 1$, the growth rate of the $n=1$ mode decreases. When the magnitude of the toroidal flow approaches the sound speed, the mode can be stabilized even though the safety factor q is less than unity. The flow twists and shears the mode over small scale lengths that are limited by the magnitude of the transport coefficients. The magnitude of the transport coefficients (resistivity and viscosity) used in the simulations must be large enough to resolve these small scale lengths. Because of the finite number of grid points in the simulations, the magnitude of the resistivity and the viscosity used in the simulations is much larger than those at the center of a hot tokamak with central Lundquist number $S \sim 10^9$. However, since the flow free growth rate of the $n=1$ mode is smaller at very small η , the magnitude of the toroidal flow required for stabilization of sawteeth is likely even smaller than that found in our simulations at larger η . The simulations demonstrate that, in addition to the current and pressure profiles, the toroidal velocity profile must be included in sawtooth stability analyses of tokamaks.

The transport coefficients in our simulations are comparable to those in colder tokamaks like the COMPASS-C tokamak.⁸ Sawteeth have been stabilized in experiments on the COMPASS-C tokamak utilizing externally applied resonant magnetic perturbations.⁸ In these experiments, a magnetic perturbation with poloidal mode number $m=2$ and toroidal mode number $n=1$ is applied to a tokamak plasma. The resonant magnetic perturbation brings the plasma to rest at the $q=2$ flux surface, producing a large increase in the

toroidal velocity shear together with the suppression of sawteeth. These observations provide evidence of the impact of sheared flows on the stability of sawteeth.

ACKNOWLEDGMENT

This research was supported by the U.S. Department of Energy.

- ¹S. von Goeler, W. Stodiek, and N. R. Sauthoff, Phys. Rev. Lett. **33**, 1201 (1974).
- ²R. J. Hastie, Astrophys. Space Sci. **256**, 177 (1997/1998).
- ³B. B. Kadomtsev, Fiz. Plazmy **1**, 710 (1975) [Sov. J. Plasma Phys. **1**, 389 (1975)].
- ⁴B. Coppi, R. Galvao, R. Pellat, M. N. Rosenbluth, and P. H. Rutherford, Sov. J. Plasma Phys. **2**, 533 (1976).
- ⁵A. Sykes and J. A. Wesson, Phys. Rev. Lett. **37**, 140 (1976).
- ⁶R. E. Denton, J. F. Drake, R. G. Kleva, and D. A. Boyd, Phys. Rev. Lett. **56**, 2477 (1986).
- ⁷D. J. Campbell, D. F. H. Start, J. A. Wesson *et al.*, Phys. Rev. Lett. **60**, 2148 (1988).
- ⁸T. C. Hender, R. Fitzpatrick, A. W. Morris *et al.*, Nucl. Fusion **32**, 2091 (1992).
- ⁹B. Coppi, R. J. Hastie, S. Migliuolo, F. Pegoraro, and F. Porcelli, Phys. Lett. A **132**, 267 (1988).
- ¹⁰R. B. White, M. N. Bussac, and F. Romanelli, Phys. Rev. Lett. **62**, 539 (1989); Phys. Fluids B **2**, 745 (1990).
- ¹¹J. A. Holmes, B. A. Carreras, and L. A. Charlton, Phys. Fluids B **1**, 788 (1989).
- ¹²G. Einaudi and F. Rubini, Phys. Fluids **29**, 2563 (1986).
- ¹³X. L. Chen and P. J. Morrison, Phys. Fluids B **2**, 495 (1990).
- ¹⁴R. G. Kleva, Phys. Fluids B **5**, 774 (1993).
- ¹⁵R. G. Kleva, Phys. Fluids B **4**, 218 (1992).
- ¹⁶F. L. Waelbroeck, Phys. Plasmas **3**, 1047 (1996).
- ¹⁷C. Wahlberg and A. Bondeson, Phys. Plasmas **7**, 923 (2000).
- ¹⁸R. G. Kleva and P. N. Guzdar, Phys. Plasmas **7**, 1163 (1999).
- ¹⁹S. T. Zalesak, J. Comput. Phys. **40**, 497 (1981).
- ²⁰Y. Kuribara, Mon. Weather Rev. **93**, 13 (1965).
- ²¹R. G. Kleva, J. F. Drake, and A. Bondeson, Phys. Fluids **27**, 769 (1984).